

Control of an Unusual Photo-Claisen Rearrangement in Coumarin Caged Tamoxifen through an Extended Spacer

Pamela T. Wong, Edward W. Roberts, Shengzhuang Tang, Jhindan Mukherjee, Jayme Cannon, Alyssa J. Nip, Kaitlin Corbin, Matthew F. Krummel, and Seok Ki Choi

ACS Chem. Biol., **Just Accepted Manuscript** • DOI: 10.1021/acscchembio.6b00999 • Publication Date (Web): 13 Feb 2017

Downloaded from <http://pubs.acs.org> on February 14, 2017

Just Accepted

“Just Accepted” manuscripts have been peer-reviewed and accepted for publication. They are posted online prior to technical editing, formatting for publication and author proofing. The American Chemical Society provides “Just Accepted” as a free service to the research community to expedite the dissemination of scientific material as soon as possible after acceptance. “Just Accepted” manuscripts appear in full in PDF format accompanied by an HTML abstract. “Just Accepted” manuscripts have been fully peer reviewed, but should not be considered the official version of record. They are accessible to all readers and citable by the Digital Object Identifier (DOI®). “Just Accepted” is an optional service offered to authors. Therefore, the “Just Accepted” Web site may not include all articles that will be published in the journal. After a manuscript is technically edited and formatted, it will be removed from the “Just Accepted” Web site and published as an ASAP article. Note that technical editing may introduce minor changes to the manuscript text and/or graphics which could affect content, and all legal disclaimers and ethical guidelines that apply to the journal pertain. ACS cannot be held responsible for errors or consequences arising from the use of information contained in these “Just Accepted” manuscripts.

1
2
3
4
5
6
7
8
9
10
11
12
13
14
15
16
17
18
19
20
21
22
23
24
25
26
27
28
29
30
31
32
33
34
35
36
37
38
39
40
41
42
43
44
45
46
47
48
49
50
51
52
53
54
55
56
57
58
59
60

Control of an Unusual Photo-Claisen Rearrangement in Coumarin Caged Tamoxifen through an Extended Spacer

*Pamela T. Wong,^{‡ab} Edward W. Roberts,^{‡c} Shengzhuang Tang,^{ab} Jhindan Mukherjee,^{ab} Jayme
Cannon,^{ab} Alyssa J. Nip,^c Kaitlin Corbin,^c Matthew F. Krummel,^{*c} and Seok Ki Choi^{*ab}*

^aMichigan Nanotechnology Institute for Medicine and Biological Sciences, ^bDepartment of
Internal Medicine, University of Michigan Medical School, Ann Arbor, Michigan 48109, United
States

^cDepartment of Pathology, University of California, San Francisco, 513 Parnassus Ave,
HSW512, San Francisco, California 94143, United States

*To whom correspondence should be addressed

Phone: (415) 514-3130; Email: matthew.krummel@ucsf.edu

Phone: (734) 647-0052; Email: skchoi@umich.edu

Abstract

The use of coumarin caged molecules has been well documented in numerous photocaging applications including for the spatiotemporal control of Cre-estrogen receptor (Cre-ERT2) recombinase activity. In this article, we report that 4-hydroxytamoxifen (4OHT) caged with coumarin via a conventional ether linkage led to an unexpected photo-Claisen rearrangement which significantly competed with the release of free 4OHT. The basis for this unwanted reaction appears to be related to the coumarin structure and its radical-based mechanism of uncaging as it did not occur in *ortho*-nitrobenzyl (ONB) caged 4OHT that was otherwise linked in the same manner. In an effort to perform design optimization, we introduced a self-immolative linker longer than the ether linkage, and identified an optimal linker which allowed rapid 4OHT release by both single-photon and two-photon absorption mechanisms. The ability of this construct to actively control Cre-ERT2 mediated gene modifications was investigated in mouse embryonic fibroblasts (MEFs) in which the expression of a green fluorescent protein (GFP) reporter dependent gene recombination was controlled by 4OHT release and measured by confocal fluorescence microscopy and flow cytometry. In summary, we report the implications of this photo-Claisen rearrangement in coumarin caged compounds, and demonstrate a rational linker strategy for addressing this unwanted side reaction.

Key words: Tamoxifen, Coumarin Cage, Photo-Claisen Rearrangement, Two-Photon Uncaging, Cre-ERT2 Recombination, Green Fluorescent Protein

1
2
3 The application of photocaging technology¹⁻³ has yielded numerous novel photoprobes that
4 have enabled the active control of molecular activities and cellular processes by light. The
5 fundamental concept behind these strategies is the temporary inactivation of a biologically active
6 molecule through the covalent attachment of a photocleavable cage molecule until the caged
7 molecule is reactivated by light exposure.² Several types of cage molecules, each distinct in their
8 structural and photochemical properties,⁴⁻⁶ have been reported, including *ortho*-nitrobenzene
9 (ONB),^{1, 7, 8} coumarin,^{9, 10} nitrobenzofuran,¹¹ and quinoline¹² chromophores. The contributions of
10 their applications have been well documented in numerous fields ranging from ion channels^{1, 13}
11 and enzymes^{14, 15} to gene expression,¹⁶ photopharmacology,^{17, 18} and controlled drug transport or
12 delivery.¹⁹⁻²¹

13
14
15
16
17
18
19
20
21
22
23
24
25
26
27
28 Recently, a number of laboratories²²⁻²⁴ including ours^{25, 26} have reported on caged forms of
29 ligands for the estrogen receptor (ER), such as tamoxifen (TAM),²⁶ 4-hydroxytamoxifen
30 (4OHT)^{25, 27} and their homologues,²²⁻²⁴ and have validated their ability to control light-inducible
31 reporter gene modifications in optogenetic models.^{23, 28} In our studies,^{25, 26} we used transgenic
32 mouse embryonic fibroblasts (MEFs) with a reporter cassette (mTmG²⁹) which contains a gene
33 for red fluorescent protein (RFP) TdTomato flanked by loxP sites (Figure 1). These MEFs also
34 constitutively express Cre recombinase fused to a modified ER that has a reduced affinity for
35 native estrogen (UbcCre-ERT2³⁰). In the absence of ER ligand, Cre-ERT2 recombinase remains
36 bound to cytoplasmic Hsp70, and the MEFs constitutively express RFP. However, upon binding
37 uncaged ligand, Cre-ERT2 dissociates from Hsp70 and is translocated to the nucleus where it
38 can then excise the Loxp-flanked gene for TdTomato from the mTmG²⁹ reporter construct,
39 resulting in the expression of a membrane-bound green fluorescence protein (GFP). We reported
40 that **1** ONB-L₁-4OHT, which is highly water soluble (≥ 20 mg mL⁻¹) and cell permeable, has the
41
42
43
44
45
46
47
48
49
50
51
52
53
54
55
56
57
58
59
60

ability to induce reporter expression with a spatial resolution sufficient for selectively marking cells.²⁵

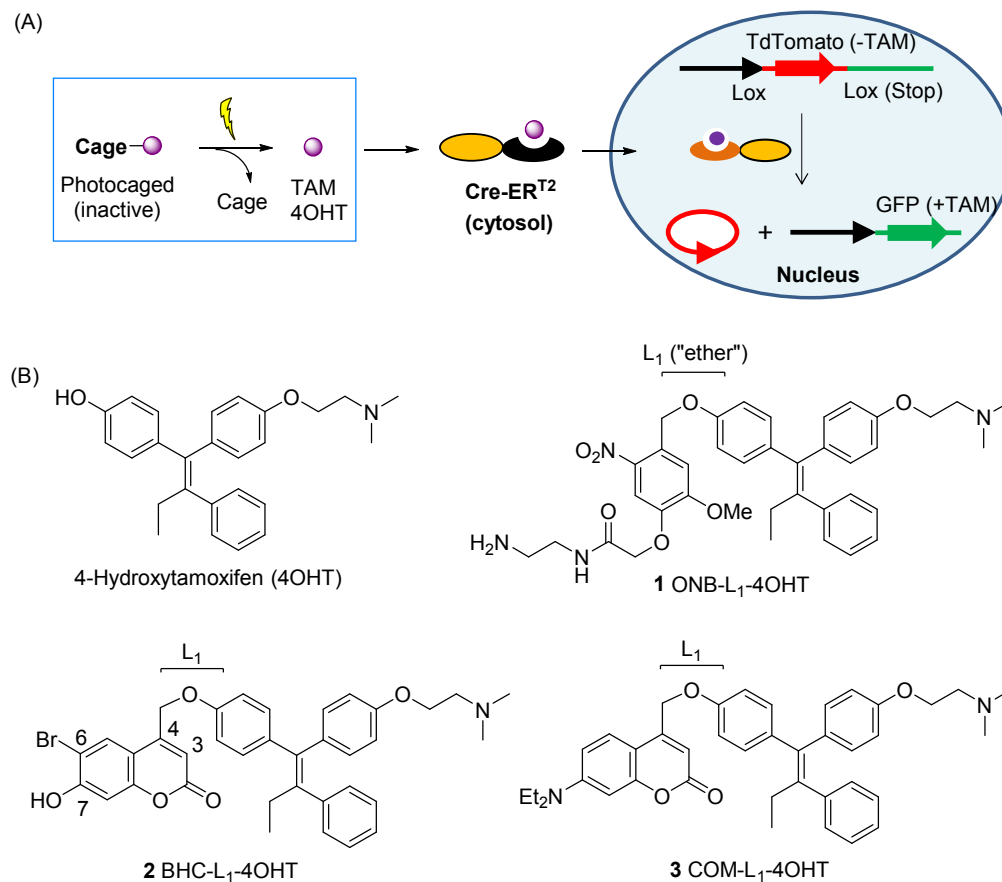


Figure 1. Photocontrol of Cre-ER mediated GFP expression. (A) Schematic for light-triggered activation of photocaged tamoxifen (TAM) or 4-hydroxytamoxifen (4OHT), and the control of reporter gene expression mediated by the Cre recombinase-estrogen receptor (ER) fusion protein. (B) Structures of 4OHT and its caged compounds including a previously reported **1** ONB-L₁-4OHT,²⁵ and two new compounds **2** BHC-L₁-4OHT, **3** COM-L₁-4OHT, each caged with BHC or COM through an ether linkage (L₁), respectively. Abbreviations: ONB = *ortho*-nitrobenzyl; BHC = 6-bromo-7-hydroxycoumarin-4-methyl; COM = 6-diethylaminocoumarin-4-methyl

1
2
3 The uncaging efficiency of tamoxifen caged compounds reported in existing Cre-ER models
4 is based on a single-photon mechanism of activation which typically occurs by absorption of
5 light in the UV range. However, the efficiency of two-photon mechanisms of activation which
6 use longer wavelength, near infrared (NIR) light remains mostly unevaluated.²⁴ Two-photon
7 uncaging of photocaged compounds occurs only on the focal plane with small cross-sections of
8 absorption,⁶ but it offers significant unique advantages over the single-photon UV activation
9 including the deeper penetration capabilities of NIR light in tissue, as well as reduced light
10 scattering and greater spatial resolution.^{6, 9} Subsequently, our current efforts focused on the
11 design and validation of new 4OHT caged compounds for their uncaging efficiency by both
12 single- and two-photon mechanisms *in vitro*.
13
14
15
16
17
18
19
20
21
22
23
24
25
26
27

28 Here, we discuss the light-controlled recombinase activity observed in the two series of
29 4OHT-caged compounds, the first based on the ONB cage including **1** ONB-L₁-4OHT, and the
30 second based on the coumarin cage which was selected for its susceptibility to one-photon
31 uncaging by UV-visible light (405–420 nm)^{7, 31, 32} as well as for its enhanced cross-sections for
32 two-photon uncaging ($\delta_{\text{uncaging}}/\text{GM} = 0.21\text{--}1.99$) compared to ONB ($\delta_{\text{uncaging}}/\text{GM} = 0.01\text{--}0.23$).⁶
33 The importance of linker selection in the design of 4OHT caged compounds was then examined.
34 Despite its important role in conjugation chemistry, the ‘linkage’ or ‘linker’ (linkage + spacer) is
35 generally less prioritized in the design of caged compounds than the cage itself because it has
36 hitherto been thought of as playing no direct role in triggering the uncaging reaction and having
37 no contribution to the wavelength selectivity of the cage. Here, we provide evidence that use of a
38 standard linker can lead to poor uncaging efficiency, as illustrated by the dramatically reduced
39 uncaging efficiency of a coumarin cage attached directly to the phenolic substrate, 4OHT
40 through an ether linkage. Specifically, use of this linkage led to the unanticipated occurrence of a
41
42
43
44
45
46
47
48
49
50
51
52
53
54
55
56
57
58
59
60

1
2
3 photo-Claisen rearrangement³³ as the major reaction path, and thus significantly reduced the
4
5 efficiency of free drug release. We demonstrate that the occurrence of such undesired reaction is
6
7 effectively blocked by application of alternative linker chemistry.
8
9

10 11 RESULTS AND DISCUSSION 12 13

14
15 **Synthesis of Coumarin Caged 4OHT via Ether Linkage.** Using a similar linker strategy
16
17 applied for ONB-based compound **1**,²⁵ we designed two coumarin caged compounds of 4OHT, **2**
18
19 BHC-L₁-4OHT and **3** COM-L₁-4OHT (Figure 1), each by tethering 4OHT (Z and E isomers) at
20
21 its phenolic moiety to a BHC (6-bromo-7-hydroxycoumarin-4-methyl)⁹ or COM (6-
22
23 diethylaminocoumarin-4-methyl)⁷ cage molecule through an ether linkage. The synthesis of **2**
24
25 and **3** was performed by direct *O*-alkylation of 4OHT with the corresponding coumarinyl-4-
26
27 methyl methanesulfonate. Each of these caged compounds was obtained with a purity of ≥95%
28
29 (UPLC) without detectable free 4OHT (Figure S6, Supporting Information). Their structural
30
31 identity was fully characterized by a combination of standard analytical methods including NMR
32
33 (¹H, ¹³C) spectroscopy (Figure S1–S5), mass spectrometry and UV–vis spectrophotometry
34
35 (Supporting Information). The exact molecular masses of **2** and **3** are in good agreement with the
36
37 experimental values measured by high resolution mass spectrometry (HRMS): calcd for **2**
38
39 C₃₆H₃₄BrNO₅ [M + H]⁺ 640.1693, found 640.1711; calcd for **3** C₄₀H₄₄N₂O₄ [M + H]⁺ 617.3374,
40
41 found 617.3373.
42
43
44
45
46
47

48
49 **Unusual Release Kinetics of **2** and **3**.** We investigated the efficiency of light-controlled
50
51 release of 4OHT from **2** by exposure to long wavelength UVA light (max intensity at 365 nm;
52
53 Figure 2). After photolysis, the exposed solutions were analyzed by thin layer chromatography
54
55 (TLC) (Figure S7), which demonstrated the rapid disappearance of **2** with the concomitant
56
57
58
59
60

1
2
3 growth of a broad spot that migrated as far as the 4OHT reference molecule. However, while
4
5 subsequent quantitative analysis performed by ultrahigh performance liquid chromatography
6
7 (UPLC) also indicated the release of 4OHT, it revealed that it was only as a minor fraction of the
8
9 total products ($\Phi_{4\text{OHT}} = 0.09$). The majority of the product consisted of a pair of closely running,
10
11 unknown products ($t_r = 10$ min) with the $\sim 1:2$ AUC (area under curve) ratio of the total of these
12
13 two peaks relative to the 4OHT peak (Figure 2C). The unknown products were isolated by flash
14
15 column chromatography, and their structural identity was assigned as **4** (Z/E isomers) based on
16
17 the combination of data from ^1H NMR spectroscopy and LC-MS mass spectrometry. Thus,
18
19 analysis of the LC-MS data indicated no change in the molecular mass ($[\text{M} + \text{H}]^+ = 640.1680$)
20
21 compared to the parent caged molecule **2** (Figure S8). The ^1H NMR spectral analysis shows
22
23 alterations broadly in 4OHT and BHC signals (Figure S9), in particular, in those from C-3 and
24
25 C-4 protons which are assigned in reference to C3- or C4-substituted coumarin compounds
26
27 (Table S1).^{34, 35} On the basis of these data, we believe that **4** was formed via the photo-Claisen
28
29 rearrangement³³ of **2** as proposed in Figure 2 with a quantum efficiency ($\Phi_{\text{Photo-Claisen}} = 0.22$)
30
31 greater than that of 4OHT release ($\Phi_{4\text{OHT}} = 0.09$). The occurrence of these unexpected products
32
33 from **2** is, in retrospect, explained by its [3,3] bond framework which is composed of an allyl
34
35 (BHC)-to-aryl (4OHT) ether, a unique structural feature required for the occurrence of photo-
36
37 Claisen rearrangement.^{33, 36}
38
39
40
41
42
43
44
45
46
47
48
49
50
51
52
53
54
55
56
57
58
59
60

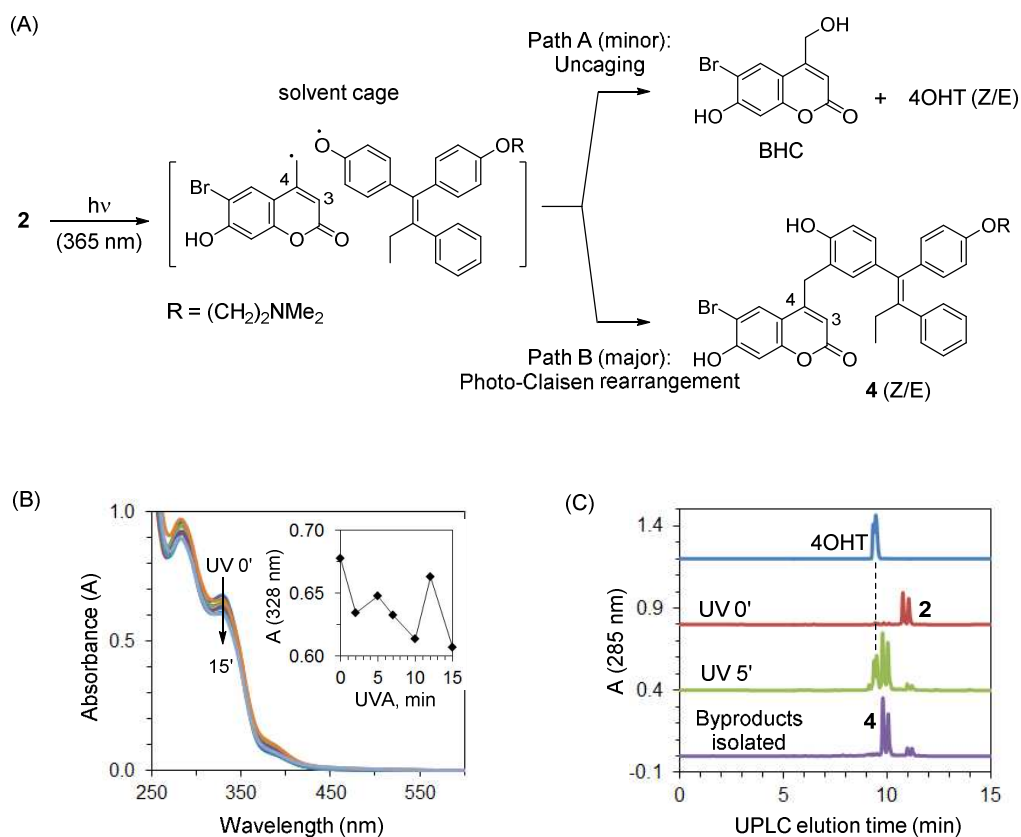


Figure 2. Mechanism of photo-Claisen rearrangement. (A) Two competing reaction paths of **2** BHC-L₁-4OHT (Z and E isomers) that occur in response to light (365 nm); path A leading to free 4OHT, and path B towards the formation of a major byproduct **4** (Z/E isomers) via photo-Claisen rearrangement. (B) Overlaid UV-vis spectra. Inset (B): a plot of absorbance at 328 nm against UV exposure time. (C) UPLC traces acquired for references and photolyzed **2** (78 μM in 20% (v/v) aqueous methanol).

However, it is noteworthy that **1** ONB-L₁-4OHT, which similarly meets a structural requirement by having an allyl (ONB)-to-aryl ether framework, did not show such byproduct formation but instead, released 4OHT predominantly as a single product ($\Phi_{4OHT} = 0.13$) in our earlier study.²⁵ We further investigated whether such differences in the product distribution between **1** and **2** are specifically inherent to the coumarin cage by performing the release study with **3** COM-L₁-4OHT, a close analogue of **2**. Its product distribution was consistent with that of

1
2
3 **2**, demonstrating 4OHT release as a minor fraction of the products ($\Phi_{4\text{OHT}} = 0.03$) along with a
4
5 larger fraction of isomeric products ($\Phi_{\text{Photo-Claisen}} = 0.05$) which are identical to **3** in their
6
7 molecular masses as characterized by LC-MS mass spectrometry ($[\text{M} + \text{H}]^+ = 617.3369$; Figure
8
9 S10). These results suggest that photo-Claisen products might occur selectively for coumarin
10
11 caged molecules, while the differences observed in quantum efficiency between BHC and COM
12
13 might be determined by the nature of the aromatic ring substituents on each coumarin cage.
14
15

16
17
18 Use of coumarin caged molecules has gained strong popularity due to their high quantum
19
20 efficiency of uncaging and broad applicability to various functional substrates.⁶ However, the
21
22 photochemical properties of the coumarin cage which are responsible for leading to a dead-end
23
24 side product instead of the desired uncaging reaction have rarely been noted except for the recent
25
26 identification of the photoisomerization of BHC caged cysteine-containing peptides (C₄-CH₂S to
27
28 C₃-S) by Distefano, et al.³⁷ and Hagen, et al.,³¹ and the photorearrangement of 4-
29
30 coumarinylmethyl phenyl ethers by Hagen and their coworkers.³⁴ Thus, our study offers strong
31
32 evidence for the broader occurrence of photorearrangement specifically in the class of coumarin
33
34 caged compounds designed with a direct ether linkage to a target molecule. It also shows that
35
36 this rearrangement reaction significantly reduces the uncaging efficiency, and suggests the need
37
38 for improving the design features in coumarin caged compounds.
39
40
41
42
43
44
45
46
47
48
49
50
51
52
53
54
55
56
57
58
59
60

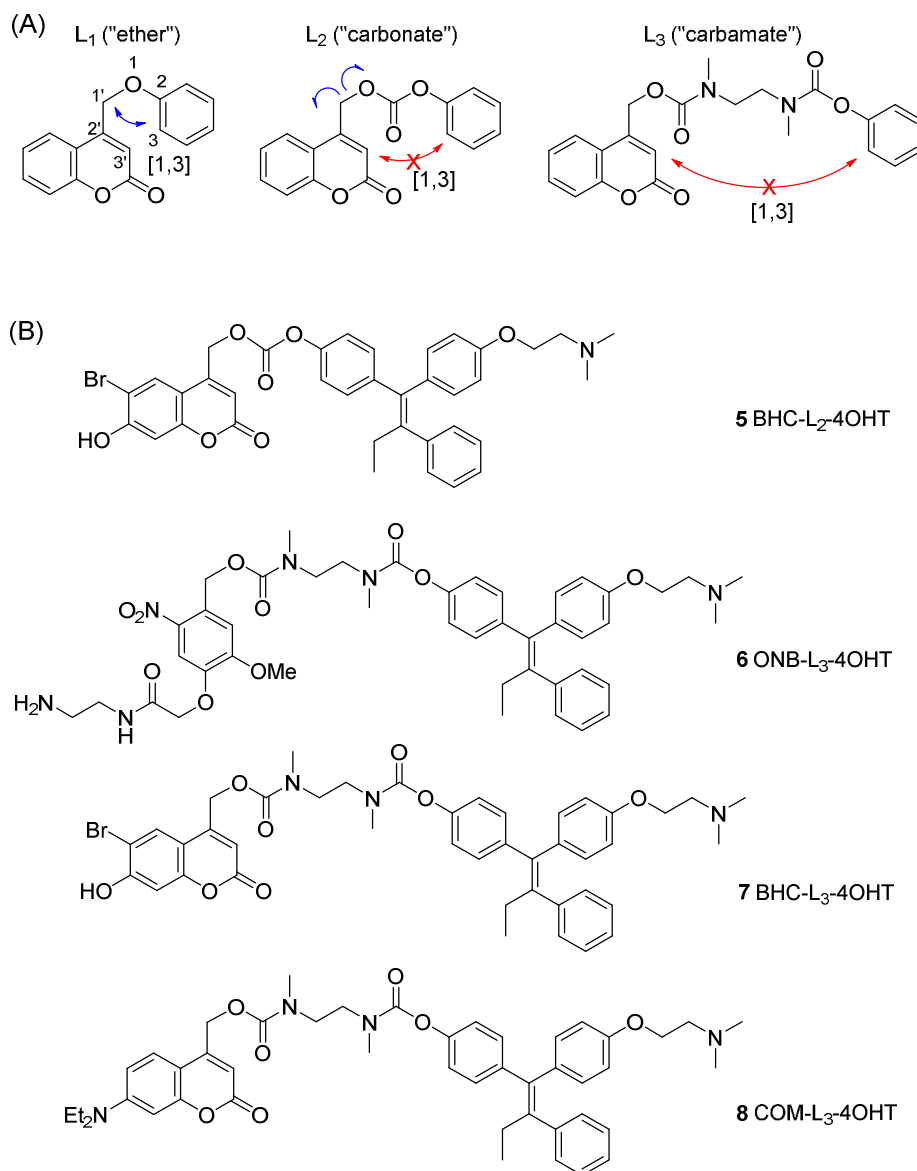


Figure 3. Design of extended spacers. (A) Release mechanism of extended linkers for coumarin-caged phenolic compounds in which photo-Claisen [1,3] rearrangement is forbidden due to lack of close proximity and self-immolation occurs instead. (B) Two linker classes used in coumarin or ONB-caged 4OHT compounds **5–8**. 4OHT is tethered to each cage molecule through a carbonate (L_2) or carbamate (L_3) linker.

Coumarin Caged 4OHT via Extended Linker. We hypothesize that the selective occurrence of photo-Claisen rearrangement in the ether-linked coumarin caged compounds is attributable to

1
2
3 the radical mechanism of C-O bond cleavage in combination with physical proximity between
4 the two radical species formed that allows recombination before they escape from their solvent
5 cage (Figure 2).³³ To circumvent such proximity-promoted photo-Claisen rearrangement, we
6 focused our design approach on extension of the linkage through either a self-immolative^{38, 39}
7 carbonate (L₂) or carbamate linker (L₃) that provides an effective physical barrier to separate two
8 radical species to be formed far enough for their escape and release. Use of these extended
9 linkers was previously reported for photocaged compounds including BHC-caged ceramides
10 (carbonate linkage),⁴⁰ ONB-caged rapamycin (carbonate),¹⁵ and ONB-caged 4OHT
11 (carbamate).²⁵ Application of these two linkers led to the synthesis of two classes of caged
12 compounds **5–8** as shown in Figure 3: (i) the carbonate-linked **5** BHC-L₂-4OHT; (ii) the
13 carbamate-linked **6** ONB-L₃-4OHT,²⁵ **7** BHC-L₃-4OHT and **8** COM-L₃-4OHT. Compound
14 homogeneity was $\geq 95\%$ for each of these caged compounds as determined by UPLC analysis
15 (Figure S6), and their structural identity was fully supported by data collected by standard
16 analytical methods as described above (Supporting Information).
17
18
19
20
21
22
23
24
25
26
27
28
29
30
31
32
33
34
35

36
37 **Release Kinetics of Extended Linkers.** We next evaluated the release kinetics of **5** BHC-L₂-
38 4OHT (125 μ M in 20% (v/v) aqueous methanol) upon exposure to UVA light (Figure S11).
39 UPLC analysis of the photolyzed solution indicated rapid release of 4OHT (73% after 2 min).
40 However, its 4OHT release was also observed in the dark (9% at 2 h), pointing to the hydrolytic
41 instability of the carbonate linkage in **5** in the aqueous solution.
42
43
44
45
46
47
48
49
50
51
52
53
54
55
56
57
58
59
60

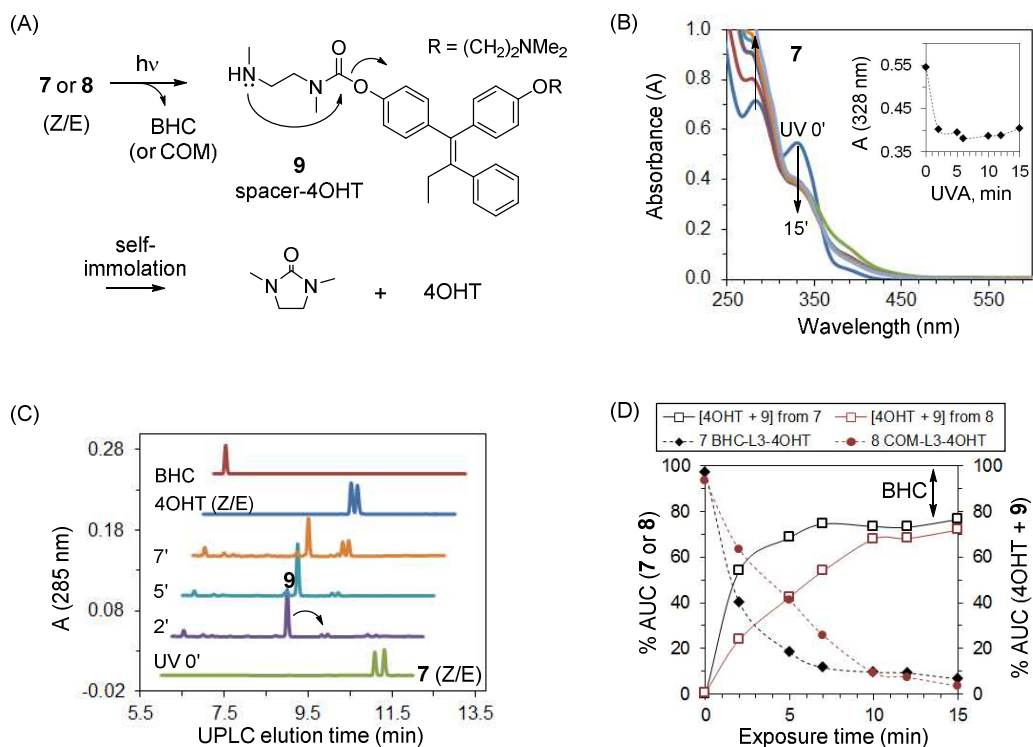


Figure 4. Release kinetics of coumarin-caged 4OHT. (A) A mechanism for the photoactivation of **7** BHC-L₃-4OHT and **8** COM-L₃-4OHT that involves cleavage to **9** spacer-4OHT, and subsequent self-immolative cyclization of **9**, resulting in release of 4OHT. (B, C) UV-vis spectra and UPLC traces obtained after the photolysis of **7** (110 μ M, 20% (v/v) aqueous methanol) as a function of exposure time. (D) A plot of the photochemical release kinetics of products (4OHT + **9**; %AUC from UPLC traces), each from **7** or **8**, respectively.

We then investigated the release kinetics of the carbamate-linked caged compounds **7** and **8**. Exposure to UVA light triggered the release of free 4OHT through formation of its carbamate derivative **9** (Figure 4, Figure S12). UPLC analysis indicates that drug release occurred in an exposure time-dependent manner and resulted in \sim 70% release of 4OHT and its direct precursor **9** after exposure for 5 min (**7**) and 10 min (**8**). 4OHT release was also confirmed by LC-MS mass spectrometric analysis which showed the appearance of a single peak corresponding to free

4OHT ($[M + H]^+ = 388.2269$; Figure S13). Regression analysis of the decay curve of **7** or **8** (%AUC, Figure 4C) over the exposure time suggests that **7** is consumed with a rate constant (first-order decay, k) of 0.343 min^{-1} which is faster than that of **8** ($k = 0.192 \text{ min}^{-1}$) at a comparable concentration. The greater decay rate of **7** is positively correlated with its higher rate of 4OHT release (Figure 4D), suggesting that its initial cleavage to **9** which is triggered by light serves as the rate determining step for the release of drug. As a consequence, the quantum efficiency of uncaging ($\Phi_{[4\text{OHT} + \mathbf{9}]}$) calculated for **7** (0.21) is higher than those of **6** (0.05) and **8** (0.07) as summarized in Table 1. This greater release efficiency suggests an advantage of using **7** over **8** as the more promising probe for two-photon activation and reporter gene expression in cells as discussed below.

Table 1. Summary of the photochemical properties of caged 4-hydroxytamoxifen (4OHT) compounds.

Cage-Linker 4OHT	(L _n)-	Linkage	λ_{max} , nm (ϵ , M ⁻¹ cm ⁻¹)	Φ^a		
				4OHT	Photo- Claisen 4	4OHT + 9
1	ONB-L ₁ -4OHT ^{ref 25}	Ether	340 (390)	0.13	nd	-
2	BHC-L ₁ -4OHT	Ether	328 (8,787)	0.09	0.22	-
3	COM-L ₁ -4OHT	Ether	394 (11,357)	0.03	0.05	-
5	BHC-L ₂ -4OHT	Carbonate	340 (6,154)	0.11 ^b	nd	-
6	ONB-L ₃ -4OHT ^{ref 25}	Carbamate	340 (317)	-	nd	0.05
7	BHC-L ₃ -4OHT	Carbamate	330 (9,990)	-	nd	0.21
8	COM-L ₃ -4OHT	Carbamate	394 (13,500)	-	nd	0.07

^a Single-photon quantum efficiency $\Phi = [dc/dt]_{\text{initial}}/[q_{n,p}(1-10^{-A})]$ where $q_{n,p}$ = photon flux ($q_p/N_A = 11.65 \times 10^{-8} \text{ mol s}^{-1}$) measured by ferrioxalate actinometry ($\Phi = 1.26$);^{41, 42} $A =$

1
2
3 absorbance at 365 nm; dc/dt = initial rate of 4OHT release or Claisen product (mol s^{-1}).^{42 b}
4
5 Contribution from non-photochemical (preexisting) hydrolysis excluded. nd = not detectable
6
7
8
9

10
11 In summary, the two extended linker classes investigated here are distinguished not only by the
12 aqueous stability of their linkages but also by their modes of achieving drug release. First, the
13 carbonate linker used in **5** shows excellent photochemical ability to release free 4OHT with a
14 decay rate greater than either of the carbamate-linked compounds, **7** or **8**. However, it lacks
15 sufficient chemical stability in aqueous solution, which is needed for precise active control. Such
16 instability is anticipated to be worse in cell media and in *in vivo* environments that contain
17 substantially higher concentrations (mM) of various nucleophilic species such as amino acids,
18 amines and protein molecules. This insufficient stability of the carbonate linkage as observed in
19 **5** was not noted previously in other caged compounds linked through a carbonate moiety to the
20 ONB¹⁵ or BHC⁴⁰ cage, indicating perhaps the involvement of other additional factors such as the
21 steric effect of the substrate molecules themselves. In contrast, the carbamate-linked compounds
22 **7** or **8** show good stability in aqueous solution with no decomposition detected for either
23 compound, at least during the entire incubation period of up to 24 h as determined by UPLC
24 analysis.
25
26
27
28
29
30
31
32
33
34
35
36
37
38
39
40
41
42
43

44
45 The mechanism of 4OHT release by **5** involves photocleavage of the $\text{CH}_2\text{-OC(=O)}$ bond
46 followed by loss of CO_2 to yield free 4OHT (Figure 3). Similarly, both **7** and **8** rely on the same
47 type of photocleavage reaction, but instead yield release of **9**, a 4OHT precursor. However, this
48 derivative subsequently undergoes intramolecular self-immolation^{38, 39} through its spacer
49 methyl(2-(methylamino)ethyl)carbamate²⁵ to release free 4OHT. Our observation that **7** shows
50 both a greater decay rate and a higher quantum efficiency of 4OHT release than **8** (Table 1,
51
52
53
54
55
56
57
58
59
60

Figure 4) clearly indicates that BHC in **7** is more effective in triggering the first photocleavage reaction than COM in **8**.

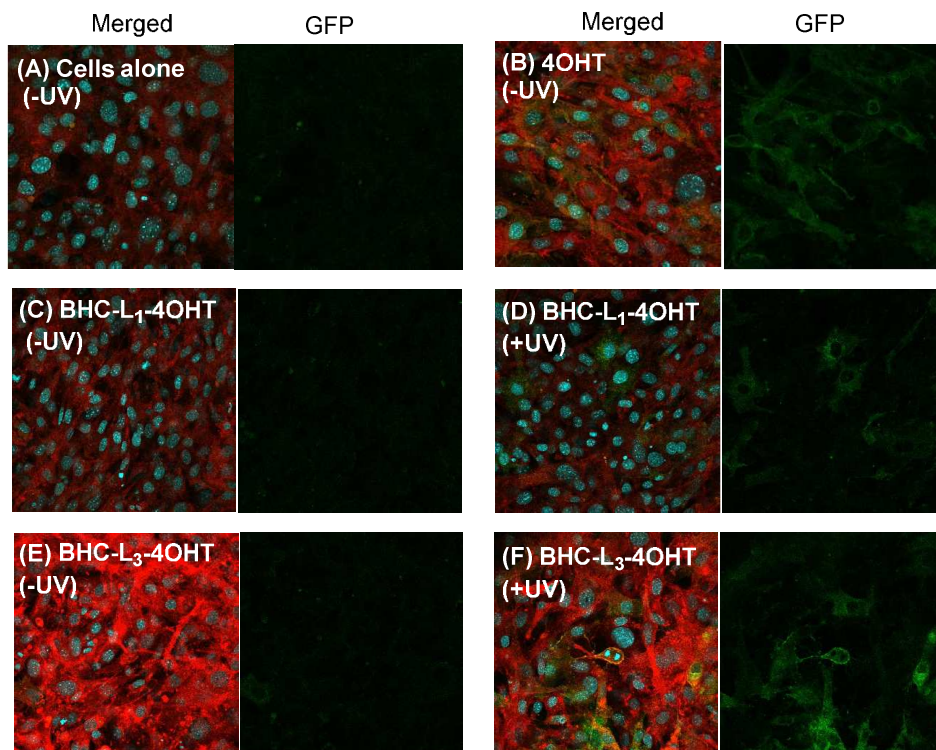


Figure 5. Confocal fluorescence microscopy analysis of the photocontrol of Cre-ERT2 mediated GFP expression in UbcCreERT2 mTmG MEF cells. As controls, MEFs were treated with (A) media alone, or (B) 4OHT without UVA exposure. MEFs were treated with **2** BHC-L₁-4OHT (C) without or (D) with UVA exposure. MEFs were treated with **7** BHC-L₃-4OHT (E) without or (F) with UVA exposure. [4OHT or caged compound] = 250 nM. UVA exposure time = 3 min. tdTomato fluorescence (red), and GFP fluorescence (green) are shown. Nuclei were labeled with DAPI (blue).

Cre-ERT2 mediated GFP expression *in vitro*. After validation of 4OHT release kinetics in solution, we selected two coumarin caged compounds **2** BHC-L₁-4OHT and **7** BHC-L₃-4OHT to compare their ability to control GFP expression in UbcCreERT2 mTmG MEF reporter cells

1
2
3 (Figure 5). This cell line constitutively expresses Cre-ERT2 from the ubiquitin promoter and
4 contains an mTmG reporter cassette which contains a loxp flanked gene for membrane bound red
5 fluorescent protein (RFP), tdTomato.^{25, 26} TdTomato is constitutively expressed. However, upon
6 Cre-ERT2 binding of free 4OHT, the loxP-flanked RFP gene is deleted by the translocated Cre
7 recombinase, and a membrane bound GFP protein is expressed instead.
8
9
10
11
12
13
14
15

16 We first examined the photocontrol of the 4OHT constructs in the modulation of such switches
17 in the expression of the reporter gene using confocal fluorescence microscopy. As similar to a
18 published protocol,²⁵ MEFs were treated with 4OHT, **2** or **7**, each at a concentration of 250 nM in
19 media and exposed to UVA light for 3 min as this exposure time falls within the middle of the
20 optimal exposure range for uncaging of all of the compounds tested (Figure 4). The cells were
21 subsequently incubated at 37°C for 24 h prior to being processed for confocal imaging. Cells
22 treated with media alone and cells treated with each caged compound in the absence of UVA
23 exposure demonstrated a lack in detectable GFP fluorescence (Figure 5). Furthermore, untreated
24 cells exposed to UVA for 3 min also showed no GFP fluorescence (Figure S14). In contrast, as a
25 positive control, MEFs were treated with free 4OHT, which led to a detectable increase in GFP
26 fluorescence even in the absence of UVA.
27
28
29
30
31
32
33
34
35
36
37
38
39
40
41
42

43 Cells treated with **2** or **7** with UVA exposure (+UVA; right), resulted in a substantial increase
44 in GFP fluorescence intensity compared to the treated cells without UV exposure (left),
45 validating UVA mediated photouncaging. However, GFP fluorescence induced by **2** appeared to
46 be weaker than that induced by **7**. While these differences between the activities of the two
47 compounds as observed by confocal microscopy are only qualitative, these results are consistent
48 with the release kinetics observed in solution where the release of free 4OHT upon UVA
49 exposure was more efficient for **7** than for **2**, the ether-linked compound that suffered from the
50
51
52
53
54
55
56
57
58
59
60

1
2
3 photo-Claisen rearrangement as the major pathway for photocleavage. In contrast, a similar
4
5 experiment with **5** BHC-L₂-4OHT (+/-UVA) indicates its potent activity in inducing GFP
6
7 expression, but with lack of UV-mediated control (Figure S14), which is consistent with its
8
9 hydrolytic instability in aqueous solutions (Figure S11). In summary, these confocal results are
10
11 supportive of the ability of 4OHT caged compounds to control the induction of GFP expression
12
13 through Cre-ERT2 recombinase activity in response to light. Our ongoing and future efforts are
14
15 focused on developing and validating an efficient method of applying the probe **7** for
16
17 spatiotemporal reporter activation *in vivo* as illustrated in Figure S15.
18
19
20
21
22
23
24
25
26
27
28
29
30
31
32
33
34
35
36
37
38
39
40
41
42
43
44
45
46
47
48
49
50
51
52
53
54
55
56
57
58
59
60

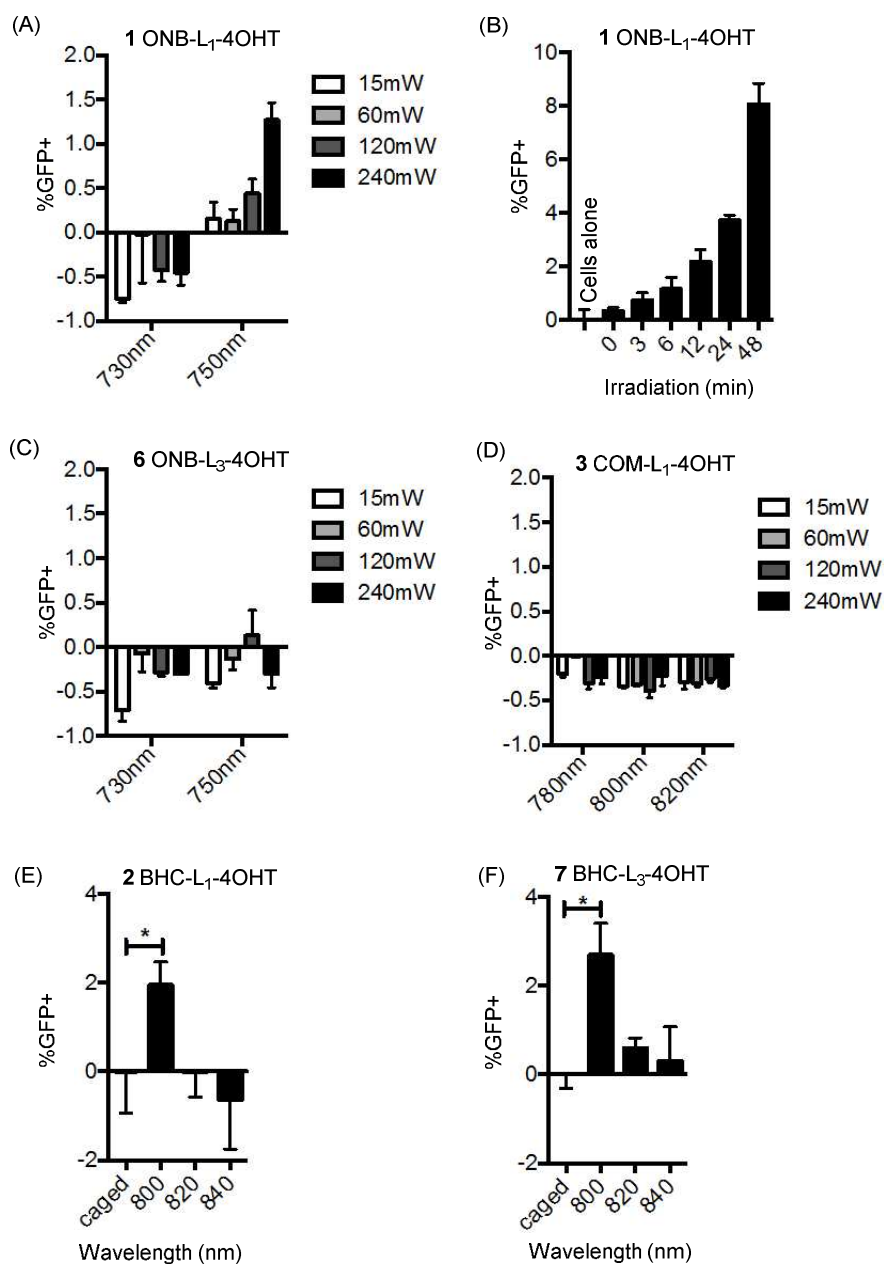


Figure 6. Two-photon activation of caged 4OHT compounds **1**, **2**, **3**, **6** and **7**. (A, C, D) Hanging drops of **1**, **3** and **6** were exposed to IR light for 10 min on the order of 5×10^{10} pulses (80 fs, 80 MHz) at different wavelengths at various powers. The uncaged compound solution was then diluted and added to UbcCre-ERT2 mTmG MEFs. At 24 h, the percent of GFP+ cells was determined by flow cytometry. Values of %GFP+ cells reported here refer to those obtained values after background correction by subtraction of the signal from cells exposed to a vehicle

1
2
3 (DMSO) which was set to 0. (B) The above process was repeated with **1** for various irradiation
4 times at 750 nm at 240 mW. (E, F) Compounds **2** and **7** were irradiated at different wavelengths
5 for 10 min at 120 mW and these were similarly used to convert reporter MEFs. The percent
6 GFP+ cells was measured by flow cytometry. [**1**] = 100 nM, [**2**] = 2.5 μ M, [**3**] = 50 nM, [**6**] =
7 200 nM, [**7**] = 250 nM. * P < 0.05
8
9
10
11
12
13
14

15 **Two-photon uncaging *in vitro*.** After validation of release kinetics by single-photon exposure,
16 we determined the efficiency by which these compounds were uncaged by two-photon excitation
17 (Figure 6). ONB groups have been reported to have narrow two-photon cross sections of
18 absorption in the 750 nm range while coumarin (COM, BHC) cages have broader two-photon
19 cross sections in the 800 nm range.⁶ This means that coumarin cages uncage more efficiently at
20 wavelengths more useful for use in tissue. As such we tested the uncaging efficiency of **1** ONB-
21 L₁-4OHT and **6** ONB-L₃-4OHT by two-photon illumination at 730 nm and 750 nm, and **3** COM-
22 L₁-4OHT by two-photon illumination at each of three different wavelengths (780 nm, 800 nm,
23 820 nm) at various laser powers. To get significant uncaging ($\geq 2\%$ GFP+) of **1**, 240 mW
24 illumination was required at 750 nm for 10 min while %GFP+ was positively correlated with the
25 irradiation time with a maximum value of $\sim 8\%$ (Figure 6A–6B). However even at this high
26 power **3** and **6** showed no appreciable uncaging (Figure 6C–6D). The efficiency of uncaging of **1**
27 could be improved by increasing the time of the exposure (Figure 6B); however at 240 mW, two-
28 photon illumination using a pulsed laser at 750 nm would damage tissues which would be
29 exacerbated by these long exposures. **1** was more efficiently activated than **6** by two photon
30 illumination consistent with the increased decay rate seen with single photon illumination.
31
32
33
34
35
36
37
38
39
40
41
42
43
44
45
46
47
48
49
50
51
52

53
54 Since **3** COM-L₁-4OHT undergoes such a significant side reaction, it is likely this lack of
55 uncaging is due to this inefficient uncaging. As such we compared the efficiency of uncaging of
56
57
58
59
60

1
2
3 BHC caged compounds **2** BHC-L₁-4OHT and **7** BHC-L₃-4OHT at wavelengths between 800 nm
4 and 840 nm (Figure 6E–6F). These uncaging experiments were performed at the concentration
5 which is either identical to that used in Cre-ERT2 mediated GFP expression (250 nM for **7**;
6 Figure 5) or higher (2.5 μM for **2**) due to its relatively low efficiency of 4OHT release. Hanging
7 drops of **2** and **7** were illuminated for 10 min at 120 mW laser power. Both **2** and **7** showed
8 uncaging activity at 800 nm, and similar to the observations made for single-photon uncaging, **7**
9 was also uncaged most efficiently by two-photon excitation. Indeed at 120 mW power for 10
10 min, **7** was 6 times more active in inducing GFP expression than **1** (2.7% GFP+ compared to
11 0.4% GFP+). The carbonate linked compound **5** was not tested for two photon uncaging as it is
12 unstable in aqueous solutions and so was as potent at inducing GFP expression with or without
13 UVA illumination (Figure S14).
14
15
16
17
18
19
20
21
22
23
24
25
26
27
28
29

30 CONCLUSION

31
32
33
34 In summary, we designed a series of new 4OHT probes caged with coumarin through the
35 extended spacer for light controlled GFP gene expression in UbcCreERT2 mTmG MEFs, and
36 validated their effective uncaging activity *in vitro* by both single- and two-photon mechanisms.
37 We believe that this study represents a significant advancement and gives new insights into the
38 development of photoprobes that enable precise control of cell labeling based on a Cre-ER
39 reporter system. Uncaging by single-photon irradiation occurred rapidly, in as short of an
40 exposure time as 2 min for both BHC and COM caged compounds, with quantum efficiency (Φ)
41 as high as 0.21 (Φ , Table 1). BHC caged compounds exhibited more effective uncaging than
42 their COM analogues. A representative compound, **7**, was activated on MEFs by UVA,
43 demonstrating its ability to temporally induce GFP reporter expression.
44
45
46
47
48
49
50
51
52
53
54
55
56
57
58
59
60

1
2
3
4
5
6
7
8
9
10
11
12
13
14
15
16
17
18
19
20
21
22
23
24
25
26
27
28
29
30
31
32
33
34
35
36
37
38
39
40
41
42
43
44
45
46
47
48
49
50
51
52
53
54
55
56
57
58
59
60

Uncaging by two-photon irradiation induced an increase in the %GFP+ cells as high as 8% for certain caged compounds (Figure 6), though this was less efficient than that observed by single-photon irradiation (UVA)²⁵. This result was anticipated due to the generally lower efficiency of uncaging by two-photon.^{5, 6} The two-photon efficiency was dependent on the structural type of the cage, with BHC (7) showing greater GFP expression than ONB (1). Such higher efficiency by BHC is attributable primarily to its higher two-photon cross-section of absorption ($\delta_{\text{absorption}}$) rather than its quantum efficiency of uncaging ($\Phi = 0.21$) which is not significantly higher than that of ONB ($\Phi = 0.13$, Table 1). In addition, two-photon factors including irradiation wavelength, intensity and exposure time made a significant contribution to the uncaging efficiency. However, due to inability for direct correlation between the two-photon and single-photon factors, systematic screening of these parameters for each compound was needed for the identification of the optimal uncaging conditions as done in this study.

We believe that this study offers rare insights into the mechanism of the photouncaging process, and has broad implications in the field of photocaging technology. Despite the extensive use of coumarin caged compounds,^{3, 6, 37} only few previous studies have indicated the occurrence of photorearrangement in caged thiols and phenols.^{31, 34, 37} Our present study reports on the prevalence of photo-Claisen rearrangement^{33, 36} in coumarin ether caged compounds, but no evidence is observed for the implication of such rearrangement in ONB uncaging which occurs exclusively via an intramolecular cyclization of its nitro group.⁶ We attribute the basis of this photorearrangement to the radical-based mechanism of coumarin uncaging in combination with the presence of an ether linkage which, due to its shorter length in nature brings the transient radical species generated by light exposure into close proximity, thus promoting their recombination.³³ We suggest the incorporation of an extended linker as an effective strategy to

1
2
3 circumvent its negative effect on uncaging efficiency. Use of this strategy enabled us to block
4
5 this rearrangement possibly by sufficiently separating the two radical species within their solvent
6
7 cages and thus preventing their recombination.
8
9

10
11 The photo-Claisen byproduct formed was not detectable by methods commonly used in this
12
13 field such as UV-vis spectrometry (Figure 2B) or by TLC analysis which had insufficient
14
15 resolution of separation (Figure S7). Instead, its detection and quantitation required the
16
17 development of a specific UPLC method that provides sufficient product resolution. Thus, this
18
19 study highlights the importance of linker development in the design of 4OHT caged compounds,
20
21 as well as in the design of other photocaged compounds, and underscores the importance of
22
23 analytical method choice for evaluating the formed products. It is notable that lack of such
24
25 precise analysis can result in inaccurate interpretation of biological activities *in vitro* and *in vivo*
26
27 as some of byproduct-like C-4 substituted coumarin compounds are associated with promiscuous
28
29 activities such as acting as ligands of estrogen receptors,⁴³ antioxidants,⁴⁴ and antiviral agents.⁴⁵
30
31
32
33
34
35

36 MATERIALS AND METHODS

37
38
39 Methods for the synthesis of caged 4OHT compounds, and analytical methods (¹H and ¹³C
40
41 NMR spectroscopy, UV-vis spectrometry, mass spectrometry, UPLC) are described in detail in
42
43 the Supporting Information and the references cited therein. Full details for release kinetics^{25, 26}
44
45 and cell studies *in vitro* (single-photon²⁵ and two-photon¹³ uncaging for induction of GFP
46
47 expression) are also provided in the Supporting Information.
48
49
50
51

52 **Supporting Information Available:** This material is available free of charge via the Internet at
53
54 <http://pubs.acs.org>.
55
56
57
58
59
60

1
2
3 **Author Contributions.** ‡These authors contributed equally: Pamela T. Wong and Edward W.
4
5
6 Roberts.

7
8 **Acknowledgment.** This work was supported in part by the National Cancer Institute, National
9
10 Institutes of Health under award 1R21CA191428. SKC acknowledges support from Michigan
11
12 Nanotechnology Institute for Medicine and Biological Sciences, University of Michigan Medical
13
14 School.
15

16
17
18
19 REFERENCES

- 20
21
22 1. Billington, A. P., Walstrom, K. M., Ramesh, D., Guzikowski, A. P., Carpenter, B. K., and
23
24 Hess, G. P. (1992) Synthesis and photochemistry of photolabile N-glycine derivatives and
25
26 effects of one on the glycine receptor. *Biochemistry* 31, 5500–5507.
27
28 2. Lee, H.-M., Larson, D. R., and Lawrence, D. S. (2009) Illuminating the Chemistry of Life:
29
30 Design, Synthesis, and Applications of "Caged" and Related Photoresponsive Compounds.
31
32 *ACS Chem. Biol.* 4, 409–427.
33
34 3. Brieke, C., Rohrbach, F., Gottschalk, A., Mayer, G., and Heckel, A. (2012) Light-Controlled
35
36 Tools. *Angew. Chem., Int. Ed.* 51, 8446–8476.
37
38 4. Yamazoe, S., Liu, Q., McQuade, L. E., Deiters, A., and Chen, J. K. (2014) Sequential Gene
39
40 Silencing Using Wavelength-Selective Caged Morpholino Oligonucleotides. *Angew. Chem.,*
41
42 *Int. Ed.* 53, 10114–10118.
43
44 5. Hansen, M. J., Velema, W. A., Lerch, M. M., Szymanski, W., and Feringa, B. L. (2015)
45
46 Wavelength-selective cleavage of photoprotecting groups: strategies and applications in
47
48 dynamic systems. *Chem. Soc. Rev.* 44, 3358–3377.
49
50 6. Klán, P., Šolomek, T., Bochet, C. G., Blanc, A., Givens, R., Rubina, M., Popik, V., Kostikov,
51
52 A., and Wirz, J. (2012) Photoremovable Protecting Groups in Chemistry and Biology:
53
54 Reaction Mechanisms and Efficacy. *Chem. Rev. (Washington, DC, U. S.)* 113, 119–191.
55
56
57
58
59
60

- 1
2
3
4
5
6
7
8
9
10
11
12
13
14
15
16
17
18
19
20
21
22
23
24
25
26
27
28
29
30
31
32
33
34
35
36
37
38
39
40
41
42
43
44
45
46
47
48
49
50
51
52
53
54
55
56
57
58
59
60
7. Goguen, B. N., Aemissegger, A., and Imperiali, B. (2011) Sequential Activation and Deactivation of Protein Function Using Spectrally Differentiated Caged Phosphoamino Acids. *J. Am. Chem. Soc.* *133*, 11038–11041.
 8. Wong, P. T., Tang, S., Cannon, J., Mukherjee, J., Isham, D., Gam, K., Payne, M., Yanik, S. A., Baker, J. R., and Choi, S. K. (2017) A Thioacetal Photocage Designed for Dual Release: Application in the Quantitation of Therapeutic Release by Synchronous Reporter Decaging. *ChemBioChem* *18*, 126–135.
 9. Furuta, T., Wang, S. S. H., Dantzker, J. L., Dore, T. M., Bybee, W. J., Callaway, E. M., Denk, W., and Tsien, R. Y. (1999) Brominated 7-hydroxycoumarin-4-ylmethyls: Photolabile protecting groups with biologically useful cross-sections for two photon photolysis. *Proc. Natl. Acad. Sci. U. S. A.* *96*, 1193–1200.
 10. Givens, R. S., Rubina, M., and Wirz, J. (2012) Applications of p-hydroxyphenacyl (pHP) and coumarin-4-ylmethyl photoremovable protecting groups. *Photochem. Photobiol. Sci.* *11*, 472–488.
 11. Momotake, A., Lindegger, N., Niggli, E., Barsotti, R. J., and Ellis-Davies, G. C. R. (2006) The nitrodibenzofuran chromophore: a new caging group for ultra-efficient photolysis in living cells. *Nat. Methods* *3*, 35–40.
 12. Li, Y. M., Shi, J., Cai, R., Chen, X., Luo, Z. F., and Guo, Q. X. (2010) New quinoline-based caging groups synthesized for photo-regulation of aptamer activity. *J. Photochem. Photobiol., A* *211*, 129–134.
 13. Pettit, D. L., Wang, S. S. H., Gee, K. R., and Augustine, G. J. (1997) Chemical Two-Photon Uncaging: a Novel Approach to Mapping Glutamate Receptors. *Neuron* *19*, 465–471.
 14. Lemke, E. A., Summerer, D., Geierstanger, B. H., Brittain, S. M., and Schultz, P. G. (2007) Control of protein phosphorylation with a genetically encoded photocaged amino acid. *Nat. Chem. Biol.* *3*, 769–772.
 15. Karginov, A. V., Zou, Y., Shirvanyants, D., Kota, P., Dokholyan, N. V., Young, D. D., Hahn, K. M., and Deiters, A. (2010) Light Regulation of Protein Dimerization and Kinase Activity

- 1
2
3 in Living Cells Using Photocaged Rapamycin and Engineered FKBP. *J. Am. Chem. Soc.* *133*,
4 420–423.
5
6
7
8 16. Ceo, L. M., and Koh, J. T. (2012) Photocaged DNA Provides New Levels of Transcription
9 Control. *ChemBioChem* *13*, 511–513.
10
11
12 17. Lerch, M. M., Hansen, M. J., van Dam, G. M., Szymanski, W., and Feringa, B. L. (2016)
13 Emerging Targets in Photopharmacology. *Angew. Chem., Int. Ed.* *55*, 2–24.
14
15
16
17 18. Velema, W. A., van der Berg, J. P., Szymanski, W., Driessen, A. J. M., and Feringa, B. L.
18 (2014) Orthogonal Control of Antibacterial Activity with Light. *ACS Chem. Biol.* *9*, 1969-
19 1974.
20
21
22
23 19. Wong, P. T., Chen, D., Tang, S., Yanik, S., Payne, M., Mukherjee, J., Coulter, A., Tang, K.,
24 Tao, K., Sun, K., Baker Jr, J. R., and Choi, S. K. (2015) Modular Integration of Upconversion
25 Nanocrystal-Dendrimer Composites for Folate Receptor-Specific Near Infrared Imaging and
26 Light Triggered Drug Release. *Small* *11*, 6078–6090.
27
28
29
30
31 20. Yang, Y., Shao, Q., Deng, R., Wang, C., Teng, X., Cheng, K., Cheng, Z., Huang, L., Liu, Z.,
32 Liu, X., and Xing, B. (2012) In Vitro and In Vivo Uncaging and Bioluminescence Imaging by
33 Using Photocaged Upconversion Nanoparticles. *Angew. Chem., Int. Ed.* *51*, 3125–3129.
34
35
36
37 21. Agasti, S. S., Laughney, A. M., Kohler, R. H., and Weissleder, R. (2013) A photoactivatable
38 drug-caged fluorophore conjugate allows direct quantification of intracellular drug transport.
39 *Chem. Commun. (Cambridge, U. K.)* *49*, 11050–11052.
40
41
42
43 22. Link, K. H., Shi, Y., and Koh, J. T. (2005) Light Activated Recombination. *J. Am. Chem.*
44 *Soc.* *127*, 13088–13089.
45
46
47
48 23. Lu, X., Agasti, S. S., Vinegoni, C., Waterman, P., DePinho, R. A., and Weissleder, R. (2012)
49 Optochemogenetics (OCG) Allows More Precise Control of Genetic Engineering in Mice
50 with CreER regulators. *Bioconjugate Chem.* *23*, 1945–1951.
51
52
53
54 24. Sinha, D. K., Neveu, P., Gagey, N., Aujard, I., Benbrahim-Bouzidi, C., Le Saux, T., Rampon,
55 C., Gauron, C., Goetz, B., Dubruille, S., Baaden, M., Volovitch, M., Bensimon, D., Vrizz, S.,
56
57
58
59
60

- 1
2
3 and Jullien, L. (2010) Photocontrol of Protein Activity in Cultured Cells and Zebrafish with
4 One- and Two-Photon Illumination. *ChemBioChem* 11, 653–663.
5
6
7
8 25. Faal, T., Wong, P., Tang, S., Coulter, A., Chen, Y., Tu, C. H., Baker, J. R., Choi, S. K., and
9 Inlay, M. A. (2015) 4-Hydroxytamoxifen probes for light-dependent spatiotemporal control of
10 Cre-ER mediated reporter gene expression. *Mol. BioSyst.* 11, 783–790.
11
12
13
14 26. Inlay, M. A., Choe, V., Bharathi, S., Fernhoff, N. B., Baker, J. R., Weissman, I. L., and Choi,
15 S. K. (2013) Synthesis of a photocaged tamoxifen for light-dependent activation of Cre-ER
16 recombinase-driven gene modification. *Chem. Commun. (Cambridge, U. K.)* 49, 4971–4973.
17
18
19
20
21 27. Shi, Y., and Koh, J. T. (2004) Light-Activated Transcription and Repression by Using
22 Photocaged SERMs. *ChemBioChem* 5, 788–796.
23
24
25 28. Madisen, L., Mao, T., Koch, H., Zhuo, J.-m., Berenyi, A., Fujisawa, S., Hsu, Y.-W. A.,
26 Garcia, A. J., Gu, X., Zanella, S., Kidney, J., Gu, H., Mao, Y., Hooks, B. M., Boyden, E. S.,
27 Buzsaki, G., Ramirez, J. M., Jones, A. R., Svoboda, K., Han, X., Turner, E. E., and Zeng, H.
28 (2012) A toolbox of Cre-dependent optogenetic transgenic mice for light-induced activation
29 and silencing. *Nat. Neurosci.* 15, 793–802.
30
31
32
33
34
35 29. Muzumdar, M. D., Tasic, B., Miyamichi, K., Li, L., and Luo, L. (2007) A global double-
36 fluorescent Cre reporter mouse. *genesis* 45, 593-605.
37
38
39
40 30. Ruzankina, Y., Pinzon-Guzman, C., Asare, A., Ong, T., Pontano, L., Cotsarelis, G., Zediak,
41 V. P., Velez, M., Bhandoola, A., and Brown, E. J. (2007) Deletion of the Developmentally
42 Essential Gene ATR in Adult Mice Leads to Age-Related Phenotypes and Stem Cell Loss.
43 *Cell Stem Cell* 1, 113-126.
44
45
46
47 31. Kotzur, N., Briand, B., Beyermann, M., and Hagen, V. (2009) Wavelength-Selective
48 Photoactivatable Protecting Groups for Thiols. *J. Am. Chem. Soc.* 131, 16927–16931.
49
50
51
52 32. San Miguel, V., Bochet, C. G., and del Campo, A. (2011) Wavelength-Selective Caged
53 Surfaces: How Many Functional Levels Are Possible? *J. Am. Chem. Soc.* 133, 5380–5388.
54
55
56
57
58
59
60

- 1
2
3 33. Galindo, F. (2005) The photochemical rearrangement of aromatic ethers: A review of the
4 Photo-Claisen reaction. *J. Photochem. Photobiol., C* 6, 123–138.
5
6
7
8 34. Schaal, J., Kotzur, N., Dekowski, B., Quilitz, J., Klimakow, M., Wessig, P., and Hagen, V.
9 (2009) A novel photorearrangement of (coumarin-4-yl)methyl phenyl ethers. *J. Photochem.*
10 *Photobiol., A* 208, 171–179.
11
12
13
14 35. Kim, S., Kang, D., Lee, C.-H., and Lee, P. H. (2012) Synthesis of Substituted Coumarins via
15 Brønsted Acid Mediated Condensation of Allenes with Substituted Phenols or Anisoles. *J.*
16 *Org. Chem.* 77, 6530–6537.
17
18
19
20
21 36. Pincock, A. L., Pincock, J. A., and Stefanova, R. (2002) Substituent Effects on the Rate
22 Constants for the Photo-Claisen Rearrangement of Allyl Aryl Ethers. *J. Am. Chem. Soc.* 124,
23 9768–9778.
24
25
26
27 37. Mahmoodi, M. M., Abate-Pella, D., Pundsack, T. J., Palsuledesai, C. C., Goff, P. C., Blank,
28 D. A., and Distefano, M. D. (2016) Nitrodibenzofuran: A One- and Two-Photon Sensitive
29 Protecting Group That Is Superior to Brominated Hydroxycoumarin for Thiol Caging in
30 Peptides. *J. Am. Chem. Soc.* 138, 5848–5859.
31
32
33
34
35 38. Amir, R. J., Pessah, N., Shamis, M., and Shabat, D. (2003) Self-Immolative Dendrimers.
36 *Angew. Chem., Int. Ed.* 42, 4494–4499.
37
38
39
40 39. Steiger, A. K., Pardue, S., Kevil, C. G., and Pluth, M. D. (2016) Self-Immolative
41 Thiocarbamates Provide Access to Triggered H₂S Donors and Analyte Replacement
42 Fluorescent Probes. *J. Am. Chem. Soc.* 138, 7256–7259.
43
44
45
46 40. Kim, Y. A., Ramirez, D. M. C., Costain, W. J., Johnston, L. J., and Bittman, R. (2011) A new
47 tool to assess ceramide bioactivity: 6-bromo-7-hydroxycoumarinyl-caged ceramide. *Chem.*
48 *Commun. (Cambridge, U. K.)* 47, 9236–9238.
49
50
51
52 41. Hatchard, C. G., and Parker, C. A. (1956) A New Sensitive Chemical Actinometer. II.
53 Potassium Ferrioxalate as a Standard Chemical Actinometer. *Proc. R. Soc. London, Ser. A*
54 235, 518–536.
55
56
57
58
59
60

- 1
2
3
4
5
6
7
8
9
10
11
12
13
14
15
16
17
18
19
20
21
22
23
24
25
26
27
28
29
30
31
32
33
34
35
36
37
38
39
40
41
42
43
44
45
46
47
48
49
50
51
52
53
54
55
56
57
58
59
60
42. Braslavsky, S. E. (2009) Glossary of terms used in photochemistry, 3rd edition (IUPAC Recommendations 2006). *Pure Appl. Chem.* 79, 293–465.
43. Kirkiacharian, S., Lormier, A. T., Chidiack, H., Bouchoux, F., and Cérède, E. (2004) Synthesis and binding affinity to human α and β estrogen receptors of various 7-hydroxycoumarins substituted at 4- and 3,4- positions. *Il Farmaco* 59, 981-986.
44. Raj, H. G., Parmar, V. S., Jain, S. C., Goel, S., Himanshu, P., Malhotra, S., Singh, A., Olsen, C. E., and Wengel, J. (1998) Mechanism of Biochemical Action of Substituted 4-Methylbenzopyran-2-ones. Part I: Dioxygenated 4-Methyl Coumarins as Superb Antioxidant and Radical Scavenging Agents. *Bioorg. Med. Chem.* 6, 833-839.
45. Hassan, M. Z., Osman, H., Ali, M. A., and Ahsan, M. J. (2016) Therapeutic potential of coumarins as antiviral agents. *Eur. J. Med. Chem.* 123, 236-255.

Table of Contents Graphic

